Vestibular contribution to motor output is also suppressed by voluntary action of the arm

Angelo Bartsch-Jimenez [1,3] **and Francisco J Valero-Cuevas** [1*,2]

[1] *Division of Biokinesiology and Physical Therapy, University of Southern California, Los Angeles, California, USA*
[2] *Biomedical Engineering Department, University of Southern California, Los Angeles, California, USA*
[3] *Escuela de Kinesiología, Facultad de Medicina, Universidad de Valparaíso, Valparaíso, Chile*

Correspondence*:
Corresponding Author
valero@usc.edu

Angelo Bartsch-Jiménez is an adjunct professor in the Department of Physical Therapy at Universidad de Valparaíso, Chile. He holds an MS in Statistics from Pontificia Universidad Católica de Valparaíso, Chile, and is currently a PhD candidate in Biokinesiology at the University of Southern California, Los Angeles, USA. His research focuses on muscle activity and neural control of movement, particularly in neurotypical and stroke populations.

Francisco Valero-Cuevas is a professor in the Departments of Biomedical, Electrical & Computer, and Aerospace & Mechanical Engineering, Computer Science, and Biokinesiology and Physical Therapy at the University of Southern California, Los Angeles, USA. His research interests lie at the interface of biology and engineering to better understand healthy and disrupted sensorimotor control, and create novel treatments, devices and biologically-inspired robots.

Keypoints

- The vestibular system is critical for correcting perturbations during voluntary movement.
- During voluntary head movements, vestibular suppression occurs to avoid undesirable self-perturbations.
- However, the contribution of the vestibular system to unperturbed voluntary arm movement remains unclear.
- We used intermuscular coherence (IMC) to measure vestibulospinal drive to neck and arm muscles while applying Galvanic Vestibular Stimulation (GVS), Sham, and No Stimulation. We compared IMC at Rest and unperturbed voluntary movement of the arm in neurotypical adults.
- Neck muscles showed increased shared neural drive at rest, only when GVS was applied. However, vestibular drive was suppressed during unperturbed voluntary isometric contractions and reaching movements of the arm.
- Vestibular drive to arm muscles did not increase when GVS was applied.
- We provide evidence that arm muscles do not receive vestibulospinal drive, excluding its contribution to unperturbed voluntary movement.

- These results could provide valuable insights into the vestibular contribution to motor impairments following neurological conditions such as stroke.

ABSTRACT

The vestibular sensory system is among the oldest and most fundamental contributors to motor behavior as it is critical to maintaining posture and balance. However, such low-level motor responses could interfere with cortically-mediated voluntary behavior that naturally involves posture and balance. Consequently, it has been proposed that—much like the inhibition of reflex responses—vestibular contributions to motor output is 'gated' (dubbed *vestibular suppression*) to avoid undesirable self-perturbations during voluntary head movements. Here we demonstrate such suppression also occurs for unperturbed voluntary arm function. Our evidence comes from comparing coherence at baseline (No Stimulation) and after Sham and Galvanic Vestibular Stimulation (GVS). Specifically, neck muscles showed shared neural drive (intermuscular coherence), which increased with GVS —but not Sham— at *Rest*. This GVS-mediated increased coherence in neck muscles, however, was suppressed during voluntary isometric contractions and reaching movements of the arm on the same side as the GVS was applied. No changes were found in pairwise intermuscular coherence during Sham (compared with No stimulation) or in arm muscles at either rest or during voluntary movement during GVS in neurotypical adults. In addition to extending vestibular suppression to unperturbed voluntary arm function, these results provide support for the common (yet unproven to our knowledge) notion that arm muscles do not receive vestibular neural drive during unperturbed voluntary movement. Moreover, these results shed light on the mechanisms that mediate competing descending outputs for voluntary function, and serve as a baseline against which to compare potential task-dependent dysregulation of vestibular-mediated output to the neck and arms in stroke and neurological conditions.

Keywords: vestibular output, voluntary reaching, galvanic vestibular stimulation

1 INTRODUCTION

The otoliths and semicircular canals are constantly sensing expected and unexpected head orientation and movement relative to space (Cullen, 2023b,a). These inputs are integrated with somatosensory and predictive self-motion signals from the brainstem, cerebellum and cortex (Cullen and Zobeiri, 2021). Such integration is essential for reflexive stabilization of gaze and posture, and accurate control of voluntary movements (Cullen, 2023a,b).

While vestibular reflexes are essential for providing robust responses to unexpected external stimuli, they could be counter-productive when they interfere or compete with motor signals for voluntary movements (Lopez and Cullen, 2024; Niyo et al., 2024). Consider how vestibular reflexes can be in competition with voluntary function when, for example, voluntary head rotations need to be ignored during reaching movements. Experimental evidence shows that these reflexes —observed as electromyographic responses to perturbations— are largely suppressed during active head movements. (Kwan et al., 2019; Cullen, 2023b,a). Notably, responses in the vestibular nuclei are suppressed (*vestibular suppression*), and occur in neck muscles during voluntary and self-initiated head movements (Cullen and Zobeiri, 2021). Importantly, vestibular suppression in leg muscles is also seen and modulated during voluntary leg movements for locomotion (Dakin et al., 2013) —presumably to avoid motor interference. On the other hand, the contribution of vestibular drive to upper extremity voluntary movement is critical for sensing our self-initiated movements relative to the environment (Cullen, 2023a). Moreover, allows us to estimate additional physical forces (e.g., coriolis and centrifugal forces) needed to plan and execute an accurate movement,

such as during reaching. Accordingly, the motor pathways controlling reaching movements demonstrate feedback-mediated responses at a minimal latency of 50ms. These responses compensate for displacements of the body and limb —relative to a reaching target— produced by externally applied perturbations as well as during self-motion (Adamovich et al., 2001; Azadjou et al., 2023). Moreover, they are reduced after unilateral vestibular lesions, excluding their emergence from the proprioceptive system (Raptis et al., 2007). In fact, the vestibular system contributes to the high-level planning of reaching movements, which is crucial for achieving accurate movement performance (Schlack et al., 2002; Klam and Graf, 2006; Azadjou et al., 2023). For example, neurons in the macaque parietal cortex show increased firing responses to vestibular signals, which are integrated with other somatosensory inputs, including proprioception, vision, and touch (Cullen, 2023b). Furthermore, the Corticospinal tract and brainstem output—from the Medial Longitudinal Fasciculus (MLF) which contains reticulo-, vestibulo- and tecto-spinal tracts—send converging and overlapping signals to the spinal cord during reaching and grasping tasks (Riddle and Baker, 2010).

The contribution of the vestibular system to voluntary movement is determined by measuring vestibulospinal drive while applying GVS. Vestibular afferents are stimulated through current applied via transmastoid surface electrodes, increasing vestibulospinal drive, without affecting proprioception and tactile sensory information (Forbes et al., 2015; Kwan et al., 2019; Cullen, 2023b).The GVS-mediated increase in vestibular drive evokes both ocular and postural responses with electromyographic responses in axial and appendicular muscles with a latency of 8 to 50ms (Forbes et al., 2015; Cullen, 2023a).

Given that upper limb movement also depends on accurate suppression of reflexes and accurate estimation of position and velocity of the body, we investigated the vestibular contribution to arm movements and whether suppression is also a mechanism to enable voluntary arm movements in humans. We hypothesize that, as in voluntary neck and leg movements, vestibular contributions to the activation of neck and arm muscles should differ between rest and voluntary movement of the arm. Understanding the role of the brainstem vestibular output in arm movements could then provide valuable insights into its contribution to motor impairments following neurological conditions such as stroke.

2 MATERIALS AND METHODS

Ethical Approval

The study conformed to the standards set by the Declaration of Helsinki, except for registration in a database. All participants gave their informed written consent to participate in this study, which was approved by the University of Southern California Internal Review Board (USC IRB: HS-17-00304).

Study participants

Seventeen right-handed individuals participated in the study (n=17; 7 males; 10 females), with a mean age of 21.5 years (ranging from 18 to 27 years), all free from pain, injury or any conditions affecting upper limb movement. Importantly, all participants were free from any neurological condition affecting control of the upper extremity (neurotypical).

Tasks

Participants performed the following tasks while sitting. *Rest*: Participants were seated with their hands resting on their lap or armrest. They were encouraged to stay relaxed and silent for 90 seconds at the beginning of the experimental procedures to collect baseline muscle activity (Fig. 1, left panel). *Voluntary*

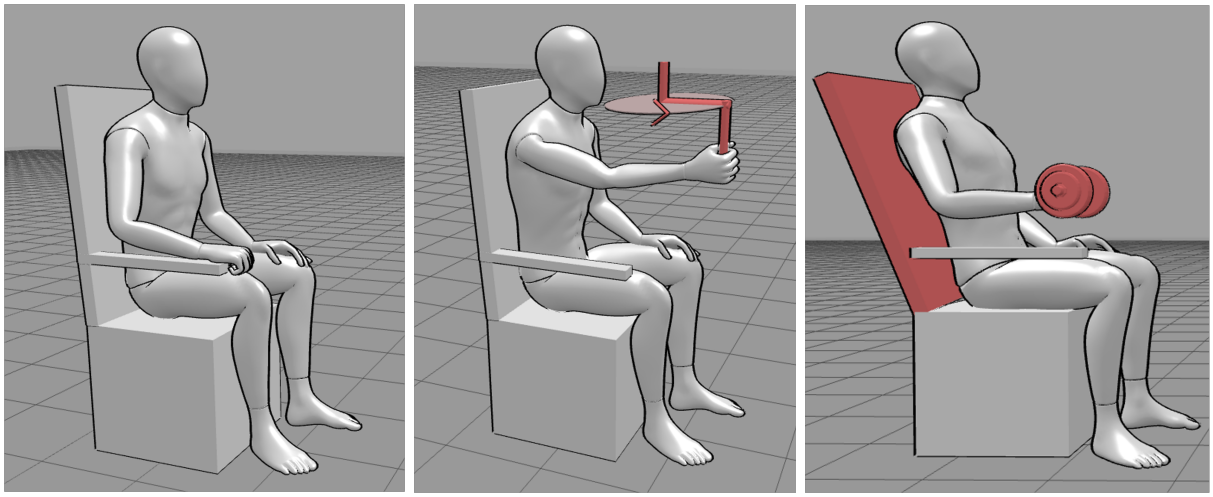

Figure 1. Tasks performed by each participant. Left: At the beginning of the experiment, each participant sat comfortably in a chair with their hands on their lap, while EMG was recorded at *Rest*. Middle: During the *Reaching* task, participants are asked to rotate an horizontal ergometer in a counterclockwise rotation with their right arm to produce a cyclical movement. Right: In the *Isometric* condition, subjects were positioned with a 15º inclined backrest, while raising their head from the headrest to activate the sternocleidomastoid muscles. Meanwhile, their right upper extremity remained unsupported as they held a 2.26kg dumbbell, with their forearm parallel to the ground and their arm aligned with the backrest.

reaching: Participants were seated in front of a hand-powered ergometer mounted to be rotated in the horizontal plane with their right arm (Fig. 1, middle panel). The protocol for this task is thoroughly described in a previous article (Laine et al., 2021). *Isometric contraction*: Participants were seated with the backrest inclined 15º backwards (Fig. 1, right panel). They were encouraged to keep their heads as close as possible to the headrest, without supporting any weight on it. This position was enforced to have a bilateral isometric contraction of the Sternocleidomastoid muscles, and Upper Trapezius for head stabilization. Simultaneously, they held a 2.26 Kg dumbbell with their hands, while their forearm is kept parallel to the ground and the arm parallel to the inclined backrest, but without any support on it. This position induced an isometric contraction of the Biceps Brachii, Anterior and Middle Deltoid muscles. Participants were encouraged to hold this position for 90 seconds, while verbal feedback was provided to correct or return to the instructed position if they departed from it. They were allowed to rest or to support their heads/extremities if they felt fatigued, however, it was not needed by any participant.

Stimulus Types

For each task, participants were subjected to three Stimulus Types; No stimulation GVS, and Sham stimulation. Based on previous protocols on human participants, GVS consisted of a binaural galvanic stimulation where the positive electrode was placed on the right mastoid process (negative electrode on the left mastoid process) (Forbes et al., 2015). The position of the electrodes was chosen to induce a vestibular response on the righ-side of the body, which was confirmed by visual inspection of the EMG signal from the SCM muscle (see Fig. 3, lower left panel). The stimulation frequency was set at 4 Hz, with an amplitude ranging between 0.8 and 1.2mA. The amplitude was modulated to avoid EMG signal saturation from the SCM muscle or if the participant felt uncomfortable. Independent of the stimulation amplitude, the Sternocleidomastoid response to GVS was always clearly visible and greater than the EMG signal at rest. For the Sham stimulation, a mechanical vibration (400 Hz) was delivered on the right mastoid (same location as the positive GVS's electrode). Each participant completed nine randomized conditions:

three Tasks (Reaching, Isometric and Rest) and three Stimulus Types (GVS, None and Sham). To mitigate potential carryover effects of GVS and Sham, the *Rest + No stimulation* condition was always completed first. Moreover, to assess the potential carryover effects of GVS, the resting condition was repeated at the end of the experiment. Subsequently, the *Rest + No stimulation* conditions at the beginning and end of the experimental procedures were compared, to determine if the vestibular drive remains increased over time, even after GVS has ceased.

Data acquisition and processing

A custom game was designed in c# to collect the angle data from the ergometer and provide live real time feedback about the user's rotation velocity (Unity3D, San Francisco, CA, USA). Custom hardware provided a pulse via an Arduino MEGA (Arduino, Somerville, MA, USA) to synchronize EMG data, angle measurements, and GVS stimuli delivery time. We collected EMG signals at 2.5 kHz from seven muscles of the right upper extremity using a DataLINK system and associated software (Biometrics Ltd, Newport, UK). Surface EMG sensors (Biometrics Ltd SX230: bipolar, gain: 1,000, bandwidth: 20–460 Hz) were placed over the right arm: Biceps Brachii (Bic), lateral head of the Triceps Brachii (Tric), Anterior, Middle and Posterior Deltoid (ADelt, MDelt, PDelt, respectively), upper Trapezius (UTrap) and Sternocleidomastoid muscles (SCM), following standard recommendations from SENIAM. Electrode placement and signal quality were confirmed using palpation of each muscle and observation of the EMG during voluntary activation. This set of muscles is sufficient for a general analysis of coupling among the shoulder/elbow muscles relevant to our task (Laine et al., 2021). All EMG signals were processed offline using R/Rstudio (R Core Team, 2021).

To remove GVS artifacts, a 10ms window surrounding each stimulus (from 2ms before to 8ms after the electrical pulse) was replaced with empty or missing values from the SCM, Deltoid (ADelt, MDelt, PDelt), and UTrap EMG signals (see Fig. 3, bottom panel). The missing data points were then interpolated to prevent aliasing and preserve the signal's frequency characteristics. Since vestibular responses have a latency of 8 to 50ms, we prevented their removal from the signals during the replacing and interpolation process. (Forbes et al., 2015). Signal processing was done according to our previous published paper (for a detailed description see Laine et al. 2021). In summary, all EMG signals were downsampled to 1,000 Hz, band-pass filtered between 8 to 250 Hz, and then full wave rectified. The filter's purpose was to remove any remaining artifacts arising from GVS, as well as from those frequencies irrelevant for intermuscular analysis. EMG rectification was done to enhance intermuscular coherence and avoid distortion of motor synchronization (Boonstra and Breakspear, 2012).

Statistical analysis

Coherence analysis measures the shared neural drive between two signals in the frequency domain (correlation in the frequency domain). As such, intermuscular coherence (IMC) assesses the degree of synchronization between the neural drive to two muscles on the basis of their EMG signals (Boonstra, 2013). Consequently, we calculated magnitude squared coherence between each muscle pair using 300 ms windows and a 50% overlap (Laine et al., 2021).

A threshold to determine significant pairwise coherence was built for easy visual inspection (see red dotted line in Fig. 4 and 5). To estimate the coherence expected by chance, we generated 1,000 phase-randomized surrogate series for each muscle pair and participant following the methods described by Ebisuzaki (1997). Coherence was calculated for each surrogate pair. A 95% confidence interval (95% CI) was constructed for each muscle pair based on the *z-transformed* coherence values obtained from the

surrogates. This interval was built across all frequency bands to provide a stringent and robust criterion for assessing statistical significance during visual inspection. Importantly, this 95% CI was not used in hypothesis testing but rather as a visual reference to highlight when individual pairwise coherence exceeds the highest values expected by chance. In other words, individual pairwise coherence above the 95% CI is likely to be significant, revealing true shared drive between the two muscles.

For unbiased statistical estimation during hypotheses testing, all raw —magnitude-squared— coherence values were transformed to *z-scores* (IMC_z) using Fisher's Z transform (IMC_z = atanh(rho)) before performing statistical comparisons (Laine et al., 2021). We compared IMC_z across the three Stimulus Types and Tasks. The values of IMC_z across the frequency spectrum were gathered into three bands: alpha (8-16 Hz), beta (16-30 Hz) and gamma (30-50 Hz) frequency bands. This approach allowed us to minimize statistical error by decreasing the number of *post-hoc* comparisons to make if the null hypothesis was rejected. Given the lack of a non-parametric alternative to test our hypotheses, a Robust Mixed Effect ANOVA model (i.e. robust repeated Measures ANOVA model) was used to test if GVS increased neural drive. The assumptions of the classical ANOVA statistical tests are not required to be met when performing these robust statistical methods. Then, if a GVS effect was found across frequency bands, we compared IMC_z using Statistical Parametrical Mapping (SPM) across the three Stimulus Types for each task separately (*Rest*, *Reaching* and *Isometric*) to identify the specific frequencies at which the differences were significant. Finally, to test for a carryover effect (i.e. long-lasting GVS effect), we compared coherence at the beginning and end of the experimental protocol when the participant was at rest and without any stimulus. Post-hoc comparisons were made using Dunnett test with Bonferroni corrections (adjusted for two comparisons: GVS vs. No Stimulation and GVS vs. Sham).

3 RESULTS

As expected, the shared neural drive between neck muscles at *Rest* (as per IMC_z) increased during *GVS* (Fig. 4). This was confirmed by a repeated measures ANOVA model with *post-hoc* comparisons and Bonferroni corrections at each frequency band (i.e., alpha to gamma, see Fig. 4 and Table 2). Importantly, no significant differences were found in IMC_z for neck muscles between None and Sham stimulus types (p-values: alpha=0.76, beta=0.7, gamma=0.55, see Table 2). This supports the notion that GVS increases vestibular output only to neck muscles (see upper panel in Fig. 4 and upper left panel in Fig. 5).

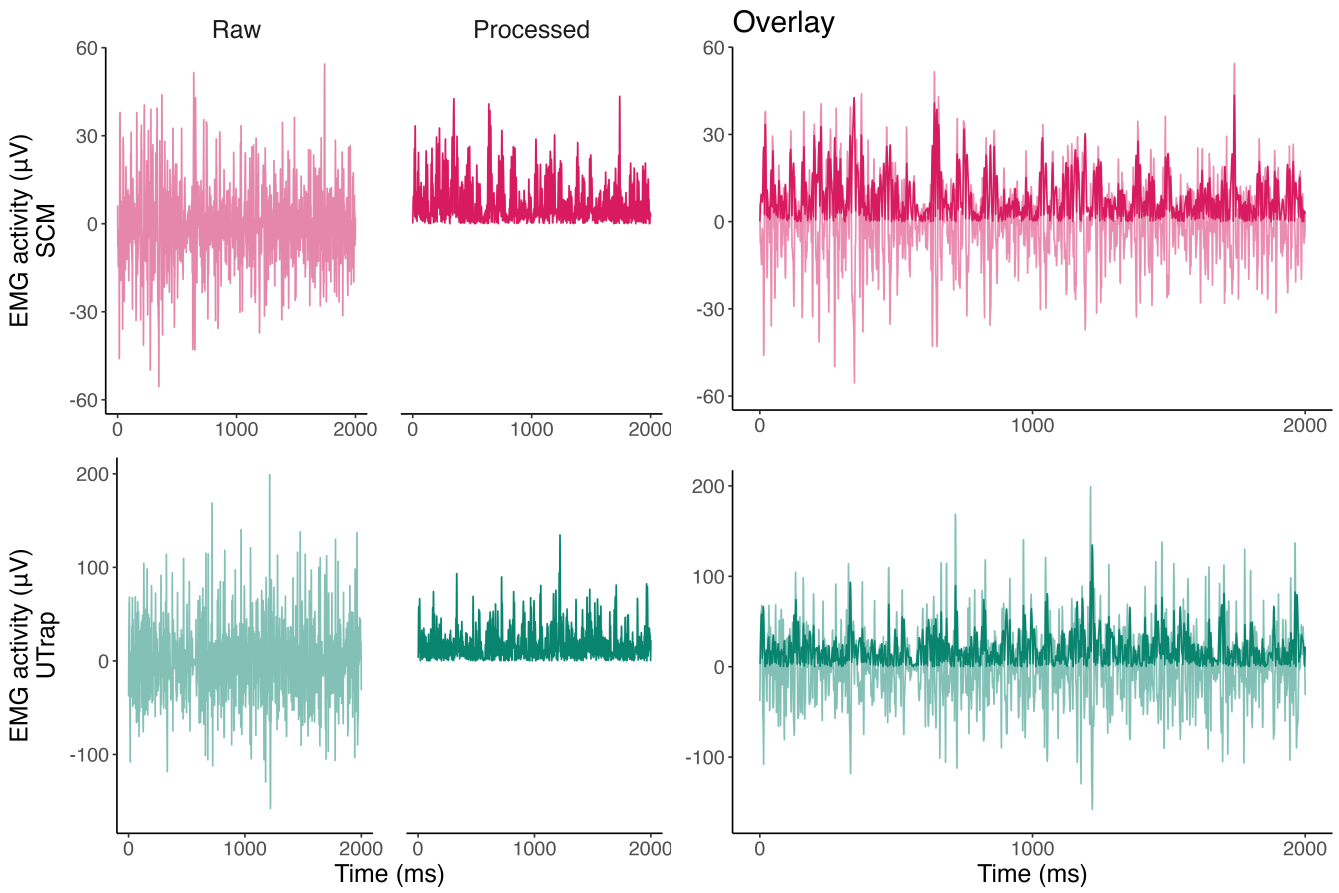

Figure 2. Raw, and processed (full-wave rectification and band-pass filtered) EMG signals from a typical participant without stimulation, recorded during the *Isometric* task, five seconds after the task started. Each trace represents 2 seconds of data. The left panel displays the *Raw* and *Processed* EMG signals for the *Sternocleidomastoid* (SCM) and *Upper Trapezius* (UTrap) muscles. The right panel overlays the signals with the sequential processing steps: the light trace corresponds to the Raw signal (see positive and negative values) and the darkest trace represents the final processed signal.

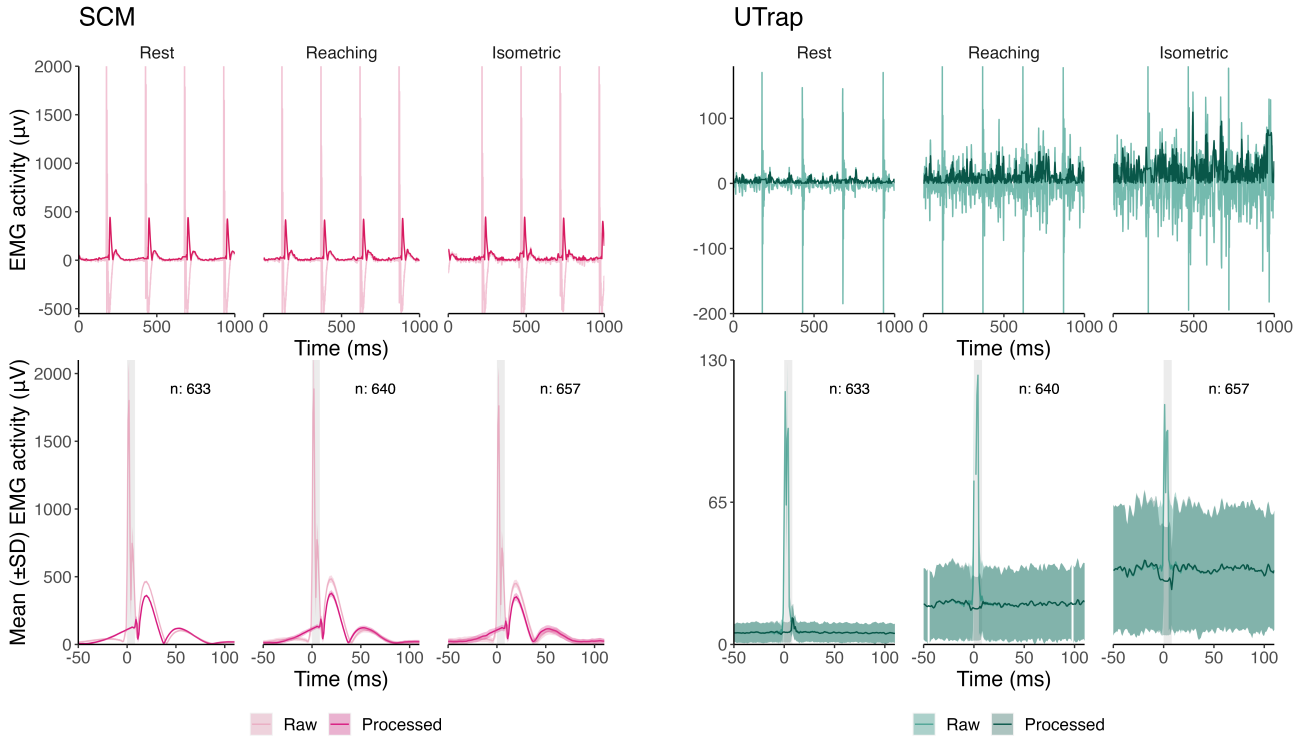

Figure 3. The *Sternocleidomastoid* (SCM) muscle shows a stereotypical response across all tasks, while the *Upper Trapezius* (UTrap), shows a smaller response restricted to *Rest*, emphasizing its suppression during Isometric and *Reaching* tasks. *Top*: Raw and Processed (GVS artifact removed, full-wave rectified and band-pass filtered) EMG activity from *Sternocleidomastoid* (SCM) and *Upper Trapezius* (UTrap) muscles during each task (when *GVS* was applied) for a typical participant. Each trace corresponds to one second of activity, which was extracted when the signal was stable (5s after the tasks started)
Bottom: Mean (±SD) Raw and Processed EMG activity (across stimuli) in response to Galvanic Vestibular Stimulation (*GVS*), from 50ms before to 110ms after the stimuli was delivered. For visualization purposes of the stereotypical response, all stimuli were aligned to their delivery time (t = 0). It showcases the averaged EMG responses across all stimuli from a single participant (number of averaged stimuli highlighted inside each plot). The light trace shows the GVS artifact while the darker trace shows the EMG after this artifact was removed and the signal processed (full-wave rectified and band-pass filtered). The shaded gray area represents the 10 ms window (ranging from -2 ms to 8 ms) during which the GVS artifact was removed prior to signal processing (see Section 2). Following this window, suppression of the UTrap response is observed during voluntary action of the arm, as opposed to SCM responses, which are always visible.

201

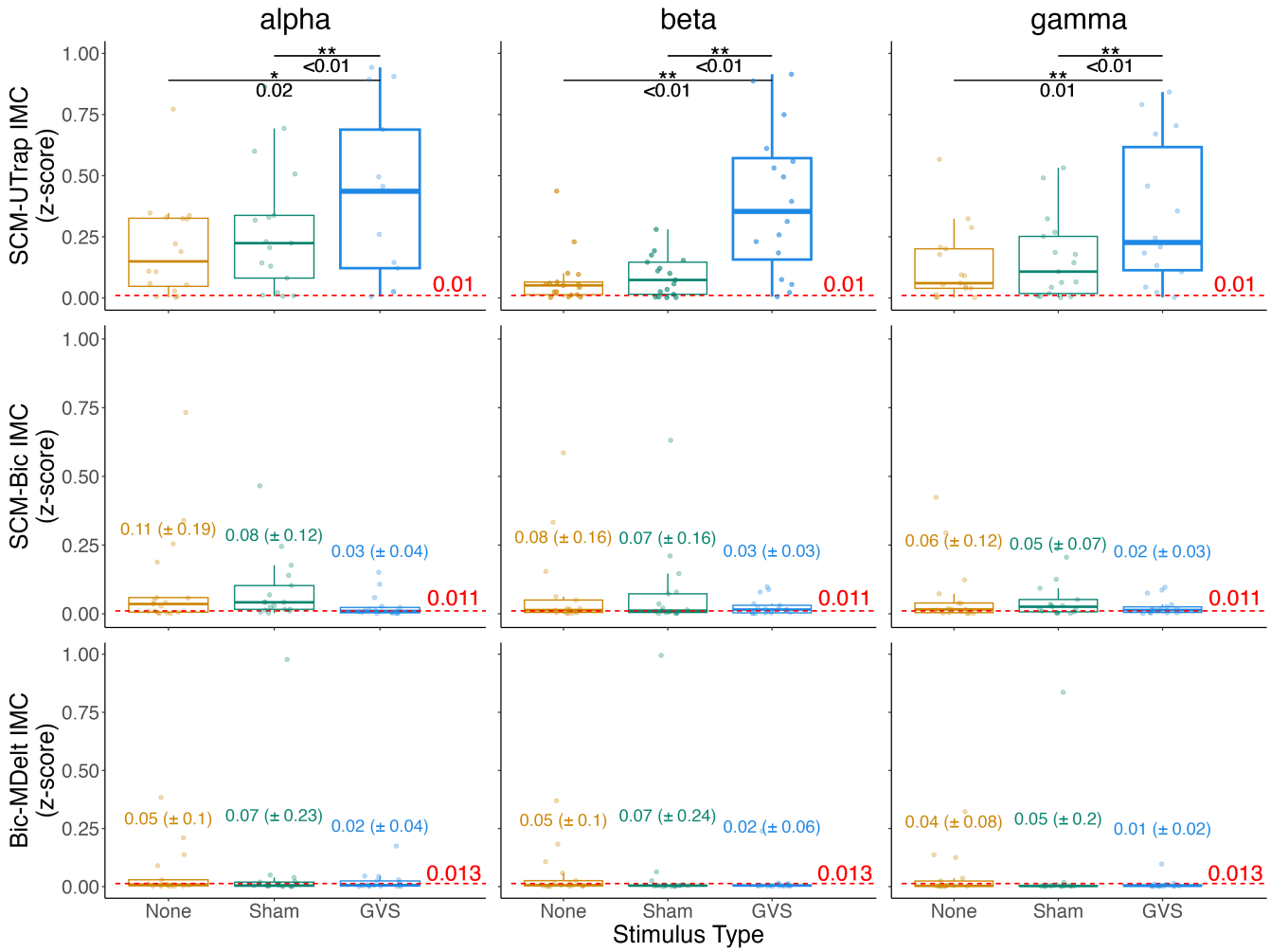

Figure 4. During Rest, Galvanic vestibular stimulation (*GVS*) increases intermuscular coherence (*IMC*) across alpha, beta and gamma frequencies between neck muscles, but not arm, muscles. We compared *z-transformed* IMC coherence across frequency bands during Rest under three different stimulus types: No Stimulation (*None*), *Sham* and GVS. Neck muscles are *Sternocleidomastoid* (SCM) and *Upper Trapezius* (UTrap). Arm muscles are *Biceps brachii* (Bic) and *Anterior Deltoid* (ADelt). Red dotted line indicates the 95% upper confidence interval estimated from 1,000 randomizations of the original signals. The middle and lower panels include the mean IMC_z across stimulus types on top of their corresponding box for easy comparison while keeping the same scales across muscle pairs.

Table 1. Robust repeated measures ANOVAs: degrees of freedom, F ratio, p-value, and effect size (η^2). Muscles: *Sternocleidomastoid* (SCM), *Upper Trapezius* (UTrap), *Biceps brachii* (Bic), *Triceps brachii* (Tric), and *Anterior, Middle, and Posterior Deltoid* (ADelt, MDelt, PDelt). Subscripts indicate Neck-Neck muscles: N-N, Neck-Arm muscles: N-A, and Arm-Arm muscles: A-A.

	alpha			beta			gamma		
Muscle	F-value (DF_1, DF_2)	p-value	η^2	F-value (DF_1, DF_2)	p-value	η^2	F-value (DF_1, DF_2)	p-value	η^2
SCM-UTrap$_{(N\text{-}N)}$	7.35 (1.5,24.6)	0.01	0.31	17.16 (1.2,19.8)	<0.001	0.52	9.35 (1.2,19.3)	<0.001	0.37
SCM-Bic$_{(N\text{-}A)}$	1.62 (1.6,25.7)	0.22	0.09	0.79 (1.8,29.4)	0.45	0.05	0.95 (1.6,26.3)	0.38	0.06
UTrap-Bic$_{(N\text{-}A)}$	1.04 (1.2,19.8)	0.34	0.06	1.07 (1.2,19)	0.33	0.06	1.09 (1.1,17.9)	0.32	0.06
UTrap-Tric$_{(N\text{-}A)}$	1.34 (1.6,25.7)	0.27	0.08	0.88 (1.2,19.5)	0.38	0.05	1.54 (2,32)	0.23	0.09
UTrap-MDelt$_{(N\text{-}A)}$	0.63 (1,16.6)	0.45	0.04	0.89 (1,16.2)	0.36	0.05	0.98 (1,16.7)	0.34	0.06
Bic-ADelt$_{(A\text{-}A)}$	1 (1.7,27.1)	0.37	0.06	1.46 (1.3,21.6)	0.25	0.08	1.43 (1.3,20.9)	0.25	0.08
Bic-MDelt$_{(A\text{-}A)}$	0.48 (1.4,23.1)	0.57	0.03	0.47 (1.4,23.1)	0.57	0.03	0.57 (1.4,22.1)	0.51	0.03
Bic-PDelt$_{(A\text{-}A)}$	0.08 (1.8,28.3)	0.90	0.00	0.01 (1.7,27.5)	0.99	0.00	0.02 (1.5,24.1)	0.95	0.00
ADelt-MDelt$_{(A\text{-}A)}$	1.09 (1.4,22.6)	0.33	0.06	0.29 (2,32)	0.75	0.02	0.66 (2,32)	0.52	0.04
ADelt-PDelt$_{(A\text{-}A)}$	0.39 (1.2,19)	0.58	0.02	0.11 (1.6,25.9)	0.85	0.01	0.28 (1.6,26)	0.71	0.02
MDelt-PDelt$_{(A\text{-}A)}$	0.1 (1.2,18.6)	0.79	0.01	0.38 (1.1,17.9)	0.57	0.02	1.14 (1.2,19.2)	0.31	0.07

Table 2. Adjusted p-values for *post-hoc* comparisons using Bonferroni corrections (adjusted for 2 comparisons). Red text indicates significant differences between stimulus types: No Stimulation (*None*), *Sham* and Galvanic Vestibular Stimulation (*GVS*). Muscles: *Sternocleidomastoid* (SCM), *Upper Trapezius* (UTrap), *Biceps brachii* (Bic), *Triceps brachii* (Tric) and *Anterior, Middle and Posterior Deltoid* (ADelt,MDelt,PDelt). Subscript indicates Neck-Neck muscles:N-N, Neck-Arm muscles:N-A, and Arm-Arm muscles: A-A.

Muscle	alpha			beta			gamma		
	None/ GVS	None/ Sham	GVS/ Sham	None/ GVS	None/ Sham	GVS/ Sham	None/ GVS	None/ Sham	GVS/ Sham
SCM- UTrap$_{(N\text{-}N)}$	<.001	0.76	0.02	<.001	0.70	<.001	<.001	0.55	0.01
SCM- Bic$_{(N\text{-}A)}$	0.12	0.69	0.08	0.22	0.96	0.24	0.22	0.75	0.18
UTrap- Bic$_{(N\text{-}A)}$	0.60	0.31	0.30	0.43	0.34	0.29	0.52	0.32	0.29
UTrap- Tric$_{(N\text{-}A)}$	0.11	0.67	0.17	0.28	0.49	0.28	0.10	0.79	0.19
UTrap-MDelt$_{(N\text{-}A)}$	0.38	0.52	0.15	0.37	0.35	0.85	0.31	0.37	0.37
Bic- ADelt$_{(A\text{-}A)}$	0.25	0.76	0.35	0.09	0.64	0.23	0.18	0.50	0.23
Bic- MDelt$_{(A\text{-}A)}$	0.27	0.80	0.45	0.34	0.72	0.44	0.19	0.79	0.40
Bic- PDelt$_{(A\text{-}A)}$	0.72	0.82	0.86	0.94	0.99	0.91	0.93	0.85	0.86
ADelt- MDelt$_{(A\text{-}A)}$	0.36	0.57	0.25	0.87	0.45	0.57	0.77	0.25	0.45
ADelt- PDelt$_{(A\text{-}A)}$	0.52	0.67	0.56	0.70	0.78	0.80	0.54	0.88	0.61
MDelt- PDelt$_{(A\text{-}A)}$	0.85	0.85	0.22	0.62	0.46	0.64	0.26	0.33	0.63

A more detailed analysis of these GVS-driven increases in IMC$_z$ between SCM-UTrap suggests such vestibular output spans a broad frequency spectrum. This was quantified by SPM analysis in 0.5 Hz bins across frequencies, which showed consistently increased IMC$_z$ during GVS when compared to None and Sham stimulus types. Specifically, IMC$_z$ was higher in the range from 12 and 50 Hz (high alpha to gamma bands, SPM$\{F\}_{2,32}$, Random Field Theory threshold=6.6, p< 0.001, Fig. 5).

A secondary analysis confirmed that our block-randomized application of the three Stimulus Types did not produce measurable carry-over effects. This was confirmed by comparing the baseline coherence of Neck muscles during *Rest* + *No stimulation* conditions at the beginning and the end of the experimental protocol (p $= 0.3$).

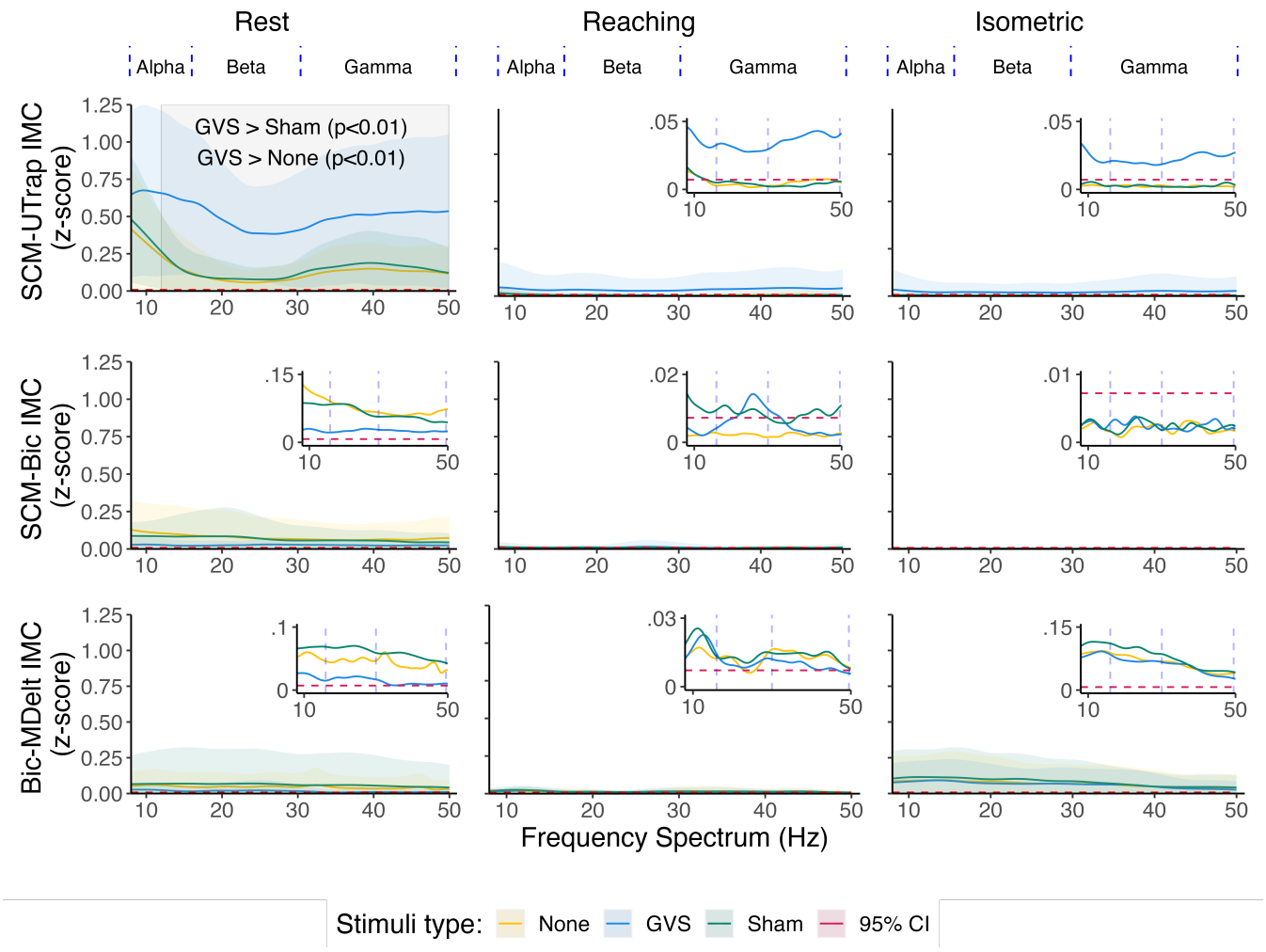

Figure 5. Galvanic Vestibular Stimulation (GVS, blue line) increases vestibular drive to neck muscles (SCM-UTrap) at Rest. However, it's suppressed during Reaching and Isometric tasks. GVS did not increase vestibular output to neck-arm and arm muscles (SCM-Bic and Bic-MDelt, respectively), neither at Rest nor during unperturbed voluntary action of the arm. No differences were found between Sham and No stimulation (which excludes a placebo effect). Mean (±SD) *z-transformed* IMC_z coherence across subjects during rest condition under three different Stimuli: No Stimulation (*None*), *Sham* and Galvanic Vestibular Stimulation (*GVS*). Each plot (except for SCM-UTrap at *Rest*) includes an inset where the signals are autoscaled. Neck muscles are SCM: *Sternocleidomastoid* and UTrap: *Upper Trapezius*. Arm muscles are Bic: *Biceps Brachii* and MDelt: *Middle Head of Deltoid*. Values above the dotted red line can be considered to have significant IMC_z, as per the 95% upper confidence interval estimated from 1,000 randomizations of the original signals. Alpha, beta and gamma frequency bands are identified by blue vertical dashed line on top of upper panel.

Interestingly, GVS did not increase IMC_z between neck muscles (SCM-UTrap) during unperturbed voluntary *Reaching* or *Isometric Contraction*. This is supported by the results of both repeated measures ANOVA and SPM analysis, which did not reveal significant differences when comparing GVS with either Sham or No stimulation (see middle and right upper panel in Fig. 5). This is an example of vestibular suppression that, to our knowledge, has not been reported during voluntary function in human or non-human primates. Finally, vestibular output is neither present nor suppressed in arm muscles in any condition (*Rest*, *Reaching* and *Isometric*), demonstrated by no significant differences in IMC_z from muscle pairs in the

active arm. This was supported by the results of both repeated measures ANOVA and SPM analysis (see middle and lower panels in Figs. 4 and 5).

4 DISCUSSION

Our intermuscular coherence results —as per IMC_z—indicate that neck, but not arm muscles, receive shared neural drive from the vestibular system (brainstem vestibular output) in neurotypical participants. Importantly, this vestibular output to neck muscles is increased at *Rest* during GVS (see upper panels in Fig. 4 and left upper panel in Fig. 5), but suppressed during voluntary action of the arm (*Reaching* and *Isometric* contraction, see middle and right upper panel in Fig. 5), without reaching statistical significance during voluntary movement of the arm. In support of this central result, we did not see increases in IMC_z during the Sham condition when compared with No stimulation. Consequently, we can exclude a tactile or proprioceptive mechanism for the changes seen during GVS, as well as a placebo effect. We propose that this is a previously unreported form of *vestibular suppression* due to voluntary action of the arm —which was known to exist in neck muscles during head movements (Cullen and Zobeiri, 2021). Moreover, the lack of increase in IMC_z with GVS between neck and arm muscles (SCM-Bic), and between arm muscles (Bic-MDelt) provides evidence that these arm muscles are unlikely to receive vestibular output at *Rest* or during unperturbed *Reaching* and *Isometric* tasks (see Figs. 4 and 5). We conclude that this previously unknown distribution and task-dependent suppression of brainstem vestibular output in neck vs. arm muscles during Rest and voluntary function sets a critical baseline in neurotypical adults. Given the clinically practical nature of GVS and EMG recordings of the arm, this baseline can be used to quantitatively assess disruptions of cortical, vestibular and brainstem output in stroke survivors.

While there are limitations in our study, we believe these do not detract from our main results or conclusions. A potential limitation of our approach is the phase-randomization method used to estimate the confidence interval for the coherence expected by chance. While this method preserves the amplitude spectrum, it may not fully account for the temporal and frequency-dependent physiological characteristics of the original signals. This could result in a null distribution for coherence that does not perfectly capture the complexities of physiological signals. We used this methods for visualization purposes only, and thus —even if we had underestimated this threshold— it does not change the interpretation of our results. Another potential limitation is that the suppression of responses during voluntary arm movements could be attributed to a lower signal-to-noise ratio (SNR). However, we believe this is unlikely, as the UTrap response is only visible during Rest, and the EMG signal drops during voluntary arm movement (see Fig. 3). Second, the noise in our signal is relatively low. For example, we observe that during Rest, the baseline activity is minimal when compared with voluntary action (see Fig. 3). Therefore, any activity above the levels of the resting condition, must be attributed to signal arising from neural drive rather than noise. This implies that vestibular drive is not clearly identified or was suppressed by neural drive originating from other cortical and subcortical sources involved in voluntary movement. Consequently, we believe the suppression of vestibular responses during voluntary action is likely due to task-related neural modulation rather than an artifact of signal-to-noise ratio. We also acknowledge that our results might be explained as a direct stimulation of neck muscles, or stimulation of the XI (or *Accesory*) cranial nerve (innervating SCM and UTrap muscles), which might be feasible due to the proximity between the GVS electrode and the neck muscles. However, it has been found that current density decreases to 10% at a distance of 10mm from stimulating surface electrodes (Enoka et al., 2020), which is a small fraction of the distance between the stimulating electrode (behind the ear) and the SCM's innervation point by the XI cranial nerve, which is 4 to 9 centimeters below the mastoid process (Bordoni et al., 2018). Moreover, we would not have seen any

vestibular suppression had such spillover stimulation short-circuited brainstem vestibular output to neck muscles. Lastly, our removal of stimulation artifacts up to 8ms. after each stimulation pulse removes, by design, the effect of such direct stimulation as well (Pinto and De Carvalho, 2008). However, this removal of the stimulation artifact every 250ms may explain the higher (and potentially artifactual) coherence below 8 Hz in Fig. 5.

Vestibular suppression during voluntary function is limited to neck muscles

Vestibular suppression in neck muscles has been previously described during active head movements across several species, including human and non-human primates (Cullen, 2023b). The purported utility is to suppress potentially counterproductive (involuntary) responses that could act as internal perturbations during voluntary movement (Cullen and Zobeiri, 2021; Cullen, 2023a). It has been proposed that vestibular suppression in neck muscles occurs when the consequences of head movement (informed by efference copy and predicted by the cerebellum) are analogous to the expected sensory information received from proprioceptors (Cullen and Zobeiri, 2021; Cullen, 2023a). Accordingly, we interpret the suppression of coherence between neck muscles (during GVS but also during no stimulation, Figure 5) as a mechanism to prevent the disruptive effect of vestibular output on head and neck kinematics during voluntary action of the arm. Case in point, our experimental design required participants to visually track a dolphin on a screen to maintain the cadence of the crank during *Reaching*, or maintain neck posture during *Isometric Contraction*. These natural tasks required active control of head and neck kinematics which could be perturbed by vestibular responses.

Vestibular output to arm muscles is absent across tasks

Vestibular output is known to affect the involuntary or reactive activation of arm muscles during perturbations of the trunk (Adamovich et al., 2001). However, our findings suggest that such vestibular-mediated adjustments are not involved or necessary during the self-initiated voluntary tasks we tested which provided stable and static trunk support. Acoustic startle studies suggest that stroke survivors exhibit greater responses on their *more-affected* (i.e. spastic-paretic) arm, presumably due to increased vestibular output (Miller and Rymer, 2017). That is, the evoked latencies were shorter and strongly lateralized in stroke survivors, which was interpreted as being triggered from vestibular instead of acoustic pathways (Miller and Rymer, 2017). Presumably, these increased vestibular-mediated responses result from the disruption of the inhibitory cortical pathways to brainstem and spine, such as those mediating vestibular projections (Miller et al., 2014; Miller and Rymer, 2017). This lack of vestibular output to arm muscles in our neurotypical participants serves as a baseline for future studies to understand the disruption of pathways affecting arm control in hemiparetic stroke.

Our results support prior reports that intermuscular coherence of vestibular origin is broadly distributed across the frequency spectrum

Intermuscular coherence in the beta band has been proposed as a biomarker that primarily reflects CST integrity, (Fisher et al., 2012; Larsen et al., 2017; Mima et al., 2001; Fang et al., 2009; Ko et al., 2023). On the other hand, the alpha band is thought to do the same for RST and propriospinal pathways (Grosse and Brown, 2003; Thevathasan et al., 2012; Tattersall et al., 2014). Our results during GVS, however, do not show a particular dominance of alpha, beta or gamma frequency bands. This supports prior work making the same inference. For example, during postural tasks, the SCM muscle has been shown to respond to stimulation with increased IMC in frequencies spanning up to 70 Hz, while lower limb muscles were coherent under 25 Hz (Forbes et al., 2015). Blouin et al. (2011) showed that during GVS, ankle muscles

—such as gastrocnemius and soleus— are coherent during the stance phase of locomotion at frequencies of around 20 Hz. Moreover, during physical activity such as running, and jumping, the frequency range of vestibular-mediated responses can increase to 70 Hz (from alpha to gamma bands)(Carriot et al., 2014; Forbes et al., 2015). In agreement with these previous findings, we found increased coherence from alpha to gamma frequency bands at Rest during GVS. Importantly, neural pathways might be reflected and overlapping across these frequency bands. For example VST and CST drive are both reflected on beta band, while RST and VST are both reflected on the alpha band. Therefore, changes in coherence on any given frequency should be interpreted carefully, specially under neurological conditions. This underscores the need to carefully interpret IMC_z in specific frequencies, particularly in stroke. That is, if the disruptions in descending pathways to the more affected arm has contributions from vestibular output, these changes in IMC_z may be reflected across a broad spectrum of frequency bands, masking decreased drive from such disrupted pathways.

In summary, our study demonstrated an increased neural drive to neck, but not arm muscles as a result of vestibular stimulation. The increased vestibular drive at rest was suppressed during isometric contraction and unperturbed voluntary reaching. These findings suggest that vestibular suppression —which has been described in head and neck muscles— also applies to voluntary arm movements. Furthermore, the absence of changes in neural drive to arm muscles during GVS provides evidence to exclude a vestibular contribution to unperturbed voluntary arm movement. Our results establish a baseline for the expected neural drive to arm and neck muscles, which could be valuable in clinical practice for quantitatively assessing disruptions of cortical, vestibular, and brainstem output in stroke survivors.

CONFLICT OF INTEREST STATEMENT

The authors declare that the research was conducted in the absence of any commercial or financial relationships that could be construed as a potential conflict of interest.

AUTHOR CONTRIBUTIONS

AB and FVC contributed to conception and design of the study. AB performed the experiments, pre-processed the data and performed the statistical analysis. AB and FVC interpreted the results and wrote the manuscript. Both authors contributed to manuscript revision, read, and approved the submitted version.

FUNDING

NSF CRCNS Japan-US 2113096, DARPA L2M Program W911NF1820264, and NIH R21-NS113613 to FVC; Division of Biokinesiology and Physical Therapy Graduate Teaching Assistantships to AB.

ACKNOWLEDGMENTS

We thank Sean Cheng and Yusuf Alvi for their help during the recruiting and testing stages of our research.

ADDITIONAL INFORMATION: DATA AVAILABILITY STATEMENT

The data that support the findings of this study are available from the corresponding author upon reasonable request.

REFERENCES

Adamovich, S., Archambault, P., Ghafouri, M., Levin, M., Poizner, H., and Feldman, A. (2001). Hand trajectory invariance in reaching movements involving the trunk. *Experimental Brain Research* 138, 288–303. doi:10.1007/s002210100694

Azadjou, H., Błażkiewicz, M., Erwin, A., and Valero-Cuevas, F. J. (2023). Dynamical analyses show that professional archers exhibit tighter, finer and more fluid dynamical control than neophytes. *Entropy* 25, 1414

Blouin, J.-S., Dakin, C. J., van den Doel, K., Chua, R., McFadyen, B. J., and Inglis, J. T. (2011). Extracting phase-dependent human vestibular reflexes during locomotion using both time and frequency correlation approaches. *Journal of Applied Physiology* 111, 1484–1490. doi:10.1152/japplphysiol.00621.2011

Boonstra, T. W. (2013). The potential of corticomuscular and intermuscular coherence for research on human motor control. *Frontiers in Human Neuroscience* 7. doi:10.3389/fnhum.2013.00855

Boonstra, T. W. and Breakspear, M. (2012). Neural mechanisms of intermuscular coherence: implications for the rectification of surface electromyography. *Journal of Neurophysiology* 107, 796–807. doi:10.1152/jn.00066.2011

Bordoni, B., Reed, R. R., Tadi, P., and Varacallo, M. (2018). Neuroanatomy, cranial nerve 11 (accessory)

Carriot, J., Jamali, M., Chacron, M. J., and Cullen, K. E. (2014). Statistics of the Vestibular Input Experienced during Natural Self-Motion: Implications for Neural Processing. *Journal of Neuroscience* 34, 8347–8357. doi:10.1523/JNEUROSCI.0692-14.2014

Cullen, K. E. (2023a). Internal models of self-motion: neural computations by the vestibular cerebellum. *Trends in Neurosciences* 46, 986–1002. doi:10.1016/j.tins.2023.08.009

Cullen, K. E. (2023b). Vestibular motor control. In *Handbook of Clinical Neurology* (Elsevier), vol. 195. 31–54. doi:10.1016/B978-0-323-98818-6.00022-4

Cullen, K. E. and Zobeiri, O. A. (2021). Proprioception and the predictive sensing of active self-motion. *Current Opinion in Physiology* 20, 29–38. doi:10.1016/j.cophys.2020.12.001

Dakin, C. J., Inglis, J. T., Chua, R., and Blouin, J.-S. (2013). Muscle-specific modulation of vestibular reflexes with increased locomotor velocity and cadence. *Journal of Neurophysiology* 110, 86–94. doi:10.1152/jn.00843.2012

Ebisuzaki, W. (1997). A method to estimate the statistical significance of a correlation when the data are serially correlated. *Journal of climate* 10, 2147–2153

Enoka, R. M., Amiridis, I. G., and Duchateau, J. (2020). Electrical Stimulation of Muscle: Electrophysiology and Rehabilitation. *Physiology* 35, 40–56. doi:10.1152/physiol.00015.2019

Fang, Y., Daly, J. J., Sun, J., Hvorat, K., Fredrickson, E., Pundik, S., et al. (2009). Functional corticomuscular connection during reaching is weakened following stroke. *Clinical neurophysiology* 120, 994–1002

Fisher, K. M., Zaaimi, B., Williams, T. L., Baker, S. N., and Baker, M. R. (2012). Beta-band intermuscular coherence: a novel biomarker of upper motor neuron dysfunction in motor neuron disease. *Brain* 135, 2849–2864. doi:10.1093/brain/aws150

Forbes, P. A., Siegmund, G. P., Schouten, A. C., and Blouin, J.-S. (2015). Task, muscle and frequency dependent vestibular control of posture. *Frontiers in Integrative Neuroscience* 8. doi:10.3389/fnint.2014.00094

Grosse, P. and Brown, P. (2003). Acoustic startle evokes bilaterally synchronous oscillatory emg activity in the healthy human. *Journal of Neurophysiology* 90, 1654–1661. doi:10.1152/jn.00125.2003

Klam, F. and Graf, W. (2006). Discrimination between active and passive head movements by macaque ventral and medial intraparietal cortex neurons. *The Journal of Physiology* 574, 367–386. doi:10.1113/jphysiol.2005.103697

Ko, N.-h., Laine, C. M., and Valero-Cuevas, F. J. (2023). Task-dependent alteration of beta-band intermuscular coherence is associated with ipsilateral corticospinal tract excitability. *Frontiers in Sports and Active Living* 5

Kwan, A., Forbes, P. A., Mitchell, D. E., Blouin, J.-S., and Cullen, K. E. (2019). Neural substrates, dynamics and thresholds of galvanic vestibular stimulation in the behaving primate. *Nature Communications* 10, 1904. doi:10.1038/s41467-019-09738-1

Laine, C. M., Cohn, B. A., and Valero-Cuevas, F. J. (2021). Temporal control of muscle synergies is linked with alpha-band neural drive. *The Journal of Physiology* 599, 3385–3402

Larsen, L. H., Zibrandtsen, I. C., Wienecke, T., Kjaer, T. W., Christensen, M. S., Nielsen, J. B., et al. (2017). Corticomuscular coherence in the acute and subacute phase after stroke. *Clinical Neurophysiology* 128, 2217–2226

Lopez, C. and Cullen, K. E. (2024). Electrical stimulation of the peripheral and central vestibular system. *Current Opinion in Neurology* 37, 40–51. doi:10.1097/WCO.0000000000001228

Miller, D. M., Klein, C. S., Suresh, N. L., and Rymer, W. Z. (2014). Asymmetries in vestibular evoked myogenic potentials in chronic stroke survivors with spastic hypertonia: Evidence for a vestibulospinal role. *Clinical Neurophysiology* 125, 2070–2078. doi:10.1016/j.clinph.2014.01.035

Miller, D. M. and Rymer, W. Z. (2017). Sound-Evoked Biceps Myogenic Potentials Reflect Asymmetric Vestibular Drive to Spastic Muscles in Chronic Hemiparetic Stroke Survivors. *Frontiers in Human Neuroscience* 11, 535. doi:10.3389/fnhum.2017.00535

Mima, T., Toma, K., Koshy, B., and Hallett, M. (2001). Coherence between cortical and muscular activities after subcortical stroke. *Stroke* 32, 2597–2601

Niyo, G., Almofeez, L. I., Erwin, A., and Valero-Cuevas, F. J. (2024). A computational study of how an α-to γ-motoneurone collateral can mitigate velocity-dependent stretch reflexes during voluntary movement. *Proceedings of the National Academy of Sciences* 121, e2321659121

Pinto, S. and De Carvalho, M. (2008). Accessory nerve stimulation: Motor response of the sternocleidomastoid muscle. *Neurophysiologie Clinique/Clinical Neurophysiology* 38, 133–136. doi:10.1016/j.neucli.2007.12.004

R Core Team (2021). *R: A Language and Environment for Statistical Computing*. R Foundation for Statistical Computing, Vienna, Austria

Raptis, H. A., Dannenbaum, E., Paquet, N., and Feldman, A. G. (2007). Vestibular System May Provide Equivalent Motor Actions Regardless of the Number of Body Segments Involved in the Task. *Journal of Neurophysiology* 97, 4069–4078. doi:10.1152/jn.00909.2006

Riddle, C. N. and Baker, S. N. (2010). Convergence of Pyramidal and Medial Brain Stem Descending Pathways Onto Macaque Cervical Spinal Interneurons. *Journal of Neurophysiology* 103, 2821–2832. doi:10.1152/jn.00491.2009

Schlack, A., Hoffmann, K., and Bremmer, F. (2002). Interaction of linear vestibular and visual stimulation in the macaque ventral intraparietal area (VIP). *European Journal of Neuroscience* 16, 1877–1886. doi:10.1046/j.1460-9568.2002.02251.x

Tattersall, T. L., Stratton, P. G., Coyne, T. J., Cook, R., Silberstein, P., Silburn, P. A., et al. (2014). Imagined gait modulates neuronal network dynamics in the human pedunculopontine nucleus. *Nature Neuroscience* 17, 449–454. doi:10.1038/nn.3642

Thevathasan, W., Pogosyan, A., Hyam, J. A., Jenkinson, N., Foltynie, T., Limousin, P., et al. (2012). Alpha oscillations in the pedunculopontine nucleus correlate with gait performance in parkinsonism. *Brain* 135, 148–160. doi:10.1093/brain/awr315